Available online at www.sciencedirect.com
SCIENCE DIRECT®
Nuclear Instruments and Methods in Physics Research B 244 (2006) 392–396
NIM B
Beam Interactions with Materials & Atoms
www.elsevier.com/locate/nimb

TRIAC: A code for track measurements using image analysis tools

D.L. Patiris [a], K. Blekas [b], K.G. Ioannides [a,*]

[a] Nuclear Physics Laboratory, Department of Physics, University of Ioannina, 451 10 Ioannina, Greece
[b] Department of Computer Science, University of Ioannina, 451 10 Ioannina, Greece

Received 13 September 2005
Available online 15 December 2005

Abstract

A computer program named TRIAC written in MATLAB has been developed for track recognition and track parameters measurements from images of the Solid State Nuclear Track Detectors CR39. The program using image analysis tools counts the number of tracks for dosimetry proposes and classifies the tracks according to their radii for the spectrometry of alpha-particles. Comparison of manual scanning counts with those output by the automatic system are presented for detectors exposed to a radon rich environment. The system was also tested to differentiate tracks recorded by alpha-particles of different energies.

PACS: 29.40.Wk; 29.30.Ep; 29.85.+c

Keywords: Solid state nuclear tracks detectors; CR39; Automatic track counting; Image analysis; Alpha-particle radioactivity

1. Introduction

Following the passage of a charged particle through a solid state nuclear track detector (SSNTD) a damage region is created usually named latent track. Latent tracks can be etched using a suitable etchant (i.e. NaOH or KOH), sufficiently enlarging them to become visible under an optical microscope (with diameters of 1 μm or more). Using the appropriate apparatus one can take images of the SSNTD's surface and count the number of the tracks. The manual counting of many images is a tedious and time-consuming task, so an automatic system is needed to speed up the process. A number of automatic track counting systems have been reported [1–5], which recognize tracks on the basis of the grey level of images.

The code presented here, TRIAC for track image analysis, is based on a segmentation method that groups image pixels in a number of grey level groups chosen by the user. After the segmentation of pixels, TRIAC counts the tracks that were recorded, even those tracks which overlap and finally classifies them according to their diameters. The analysis of an image with a PC (Intel Pentium III processor running at 600 MHz) takes 2–5 min, depending on the number of observed tracks and the digital analysis of the image. As an application, the system was used to measure activities of radon and its daughters for dosimetry purposes and also to classify tracks according to their radii.

2. Description of the algorithms used for the automatic detection of tracks

Code TRIAC was written in the high level language MATLAB, which is accompanied by many tools for special applications. The algorithm performs image segmentation, the process that groups image pixels together, based on attributes such as their intensity, location, texture features, etc. A variety of methods have been proposed for image segmentation, such as edge-based or region-based methods [6]. Amongst them, histogram-based clustering methods have been proved very effective, since they basically correspond to clustering approaches. A well known clustering method is the *K-means* algorithm [7], which tries to

* Corresponding author. Tel.: +30 2651098545; fax: +30 2651098692.
E-mail address: kioannid@cc.uoi.gr (K.G. Ioannides).

0168-583X/$ - see front matter © 2005 Elsevier B.V. All rights reserved.
doi:10.1016/j.nimb.2005.10.026

appropriately adjust the K cluster centers in order to minimize the distance from each data point to its nearest center. In the available track data, the resulting images contain, apart from the background (light pixels) and the track regions (dark pixels), pixel regions with a middle level of brightness (grey pixels). To capture the grey level pixels into the image model used for subsequent analysis, we have used $K = 3$ or 4 as the number of clusters for the clustering procedure.

Following image segmentation, pixels are labelled according to the cluster they belong to (1 for dark, 2 and more for grey light levels). Since we are mainly interested in the pixels related to the track regions, we produce a binary image from the segmented image by setting zero (0) to all pixels associated with labels 2 or higher. Furthermore, a morphological operator is performed to remove small objects whose number of interconnected pixels is less than a threshold value P (during our experiments, we have used $P = 20$). Fig. 1 provides an example of the above image analysis steps.

In this stage, the problem is reduced to counting the number of tracks in the isolated objects in the resulting binary image. The discovered objects may represent one or more overlapping tracks. For each object, the edges are found using the Canny edge detection algorithm [8], performed in two passes, one carried out with values only from pixels on a horizontal line adjacent to the central pixel, and the other executed with values only from pixels on a vertical line.

Seeing that the tracks are almost circular, the Hough transform is then applied [9], a technique to automatically detect the number of circles contained in each object. In particular, a three-dimensional Hough space is constructed. The generalized circular Hough transform requires a three-dimensional space, since three parameters are required to define a circle (the x, y coordinates of the center and the radius). Each point in the real-space image produces a peak into the Hough space, corresponding to all of the circles of various radii and center positions that could be drawn through the point. Once a cone is detected and a circle is 'recognized' at a particular point, nearby points are excluded as possible circle centers to avoid repeated detection of the same circular feature. Finally, the number of circles found corresponds to the number of tracks inside the object. An example of this process is presented in Fig. 2. It must be noticed that in the above

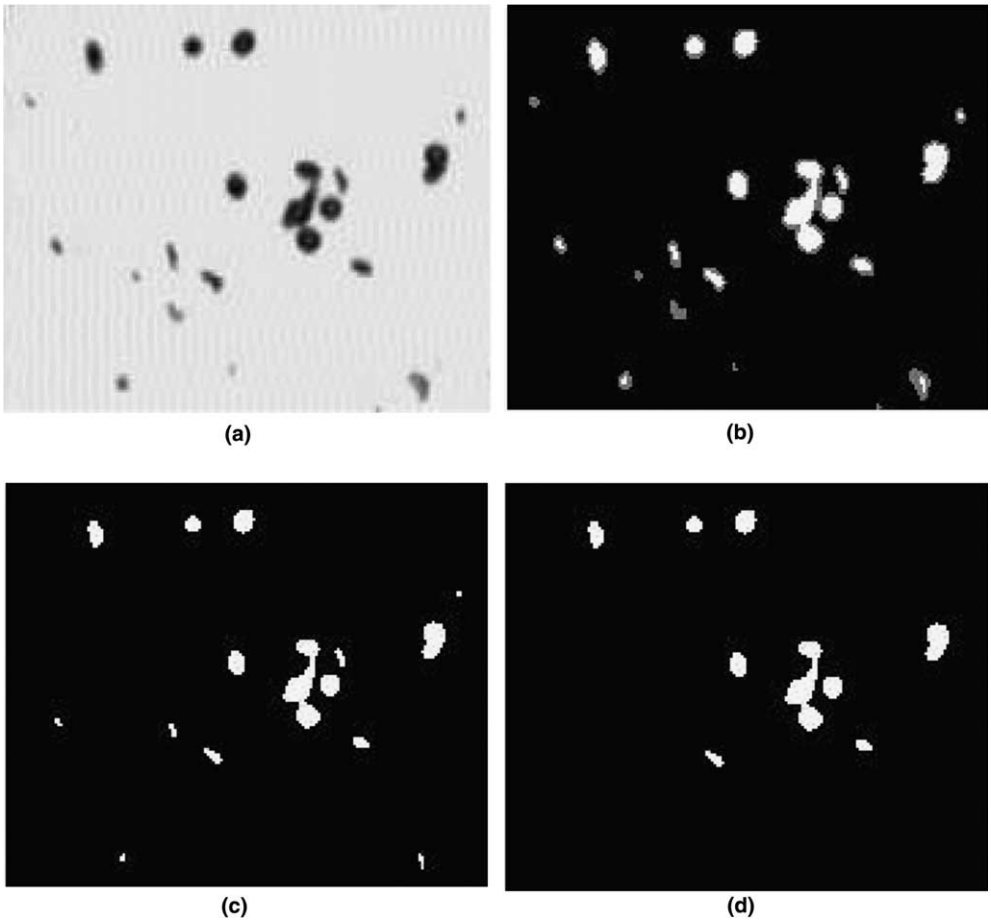

Fig. 1. The three main steps of track image analysis. The resulting corrected binary image (d) is finally used for counting the tracks: (a) original track image, (b) segmentation result: clustering the pixels into three segments (background, middle, track), (c) morphological correction: small track regions are removed and (d) binary image: only the track regions are visible.

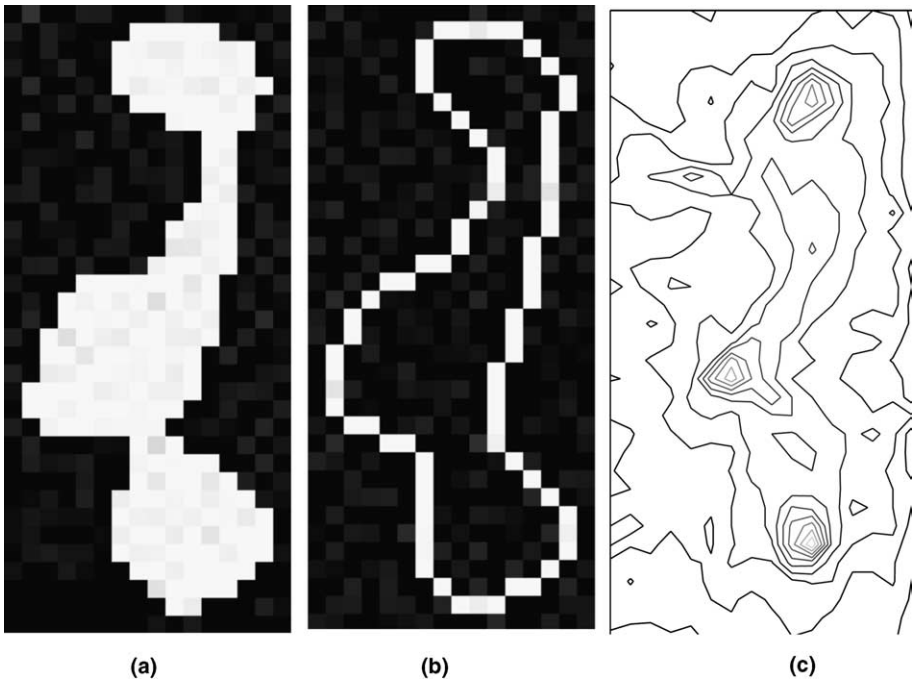

Fig. 2. Automatic tracks detection: (a) for an object first we obtain the edges image and (b) using the Canny edge detection algorithm. The application of the Hough transform detects three tracks, since the accumulator function in the Hough space (c) has three major peaks.

scheme, the gradient information of each edge pixel was used to decompose the parameter space and reduce the computational complexity [10].

3. The experimental set-up

The track measurements were carried out with CR-39 SSNTDs. To test the performance of the program two trial experiments were performed. In the first trial, the counting capacity of the code was tested. A number of CR-39 detectors were exposed in a radon chamber containing a 2000 Bq source of ^{226}Ra for 1–7 days. Due to the different exposure times, different numbers of tracks per optical field were produced (in the order of 10–10^3). The second experiment aimed to test if TRIAC could differentiate tracks recorded by alpha-particles of different energies. For this trial, plates of CR-39 were exposed to alpha-particles from a ^{241}Am source in vacuum. A collimator was placed in front of the source and polyethylene absorbers were used to reduce the energy of the alpha-particles and produce beams of different energies. These energies were precisely measured by alpha spectrometry, using a 600 mm^2 surface barrier detector.

Following exposure, the detectors were etched in a solution of 6 M NaOH at 75 °C for 8 h in the first experiment and for different etching times, ranging from 6 h to 12 h in the second experiment to remove layers of different thickness from the detector's surface. The thickness of the removed layers were measured with a digital pachymeter. Then a number of images of the detectors' surfaces were captured with the use of a microscope – video camera – frame grabber – computer recording arrangement. The images of the optical fields were taken using a 4X lens for the first experiment and were saved in 'jpg' format with 640×480 resolution. For the second experiment, a 10X lens was used and the images were also saved in 'jpg' format but with higher (1600×1200) resolution.

4. Results and discussion

To assess the counting performance of the TRIAC program, the images of tracks taken in the first experiment, were counted in two ways. First, the computer program TRACKA [11] was used to "manually" count the number of tracks per optical field with the help of the computer mouse and second TRIAC automatically enumerated the tracks. In the case of manual counting, the reliability of the results is strongly dependent on the user's experience and decreases when the number of the overlapping tracks increases. When counting with TRIAC, the user has only to enter the number of clusters and to adjust (if it is needed) the threshold value of the morphological operator. All following procedure is fully automated, the overlapping tracks are also counted in a systematic way and the results are not dependent on the user's counting skill. In Fig. 3, after choosing 3 and 4 as the number of clusters, the corresponding results are compared. In these results there is agreement between 'manual' and automated counts, expressed by a linear functional form with good correlation ($r^2 = 0.99$).

One of the challenges, which attracted significant attention in the past, is the formal description of the tracks'

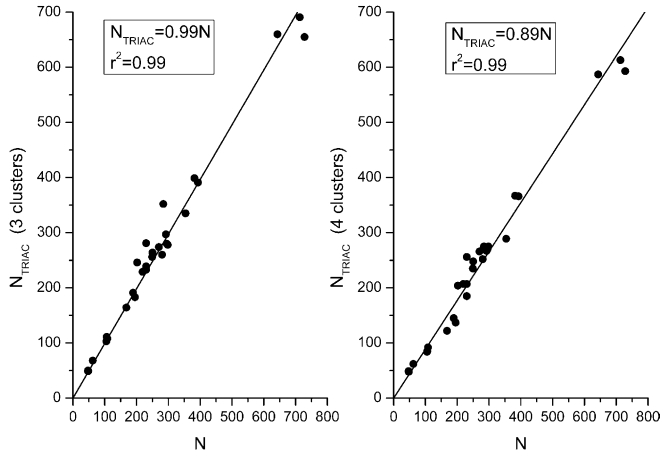

Fig. 3. The counting results, choosing of 3 and 4 as the number of the clusters for the clustering procedure. On the X axis are the manually counting results (N), while on Y axis are results counted by TRIAC (N_{TRIAC}).

growth during the chemical etching procedure. The geometry of the track development has been considered by a number of authors [12–22]. Generally, the shapes of the tracks are elliptical and the parameters of the minor and the major axis depend on the energy and the angle of incidence of the particles. In the special case of normal incidence, the shapes of the tracks are circular and their radii are strongly dependent on etching times and energy of particles. As the duration of chemical etching increases, the thickness of the removed layer and the openings of the tracks also increase. Moreover, the dependence of the tracks' diameters on the energy of alpha-particles is not linearly correlated with the thickness of the removed layers, according to theoretical models [13,16,21,22].

Using a ^{241}Am source and foils of polyethylene as absorbers, CR39 plates were exposed to four beams of different alpha-particle energies. Normal incidence was ensured by the collimator. In Fig. 4 these beams are shown as measured by an alpha spectrometer with a 600 mm^2 surface barrier detector. The radii of the alpha-particle tracks were then classified by TRIAC. In Fig. 5, typical histograms of the tracks' diameters are shown for 8 h of chemical etching. Using a calibration grid (Neubauer Improved), one pixel was found to correspond to 0.42 μm with the magnification of a 10× lens and a digital image analysis of 1600 × 1200. Comparison of the data shown in Figs. 4 and 5 indicates a relationship between the radii of the tracks and the energy of the alpha-particles.

To elaborate on the previous observation, the distribution of the tracks' radii was measured using TRIAC for different chemical etching times (from 6 h to 12 h). The experimental results for the diameters of the tracks openings are shown in Fig. 6 together with the predictions of theoretical model described by Nikezic and Yu [21], while the results of other models by Somogyi and Szalay [13], Fromm et al. [16] and Fews and Henshaw [22] are also similar for normal incidence. From the comparison of the theoretical and experimental data it was seen that the use of TRIAC straightforwardly verified the prediction of the models on the growth of tracks.

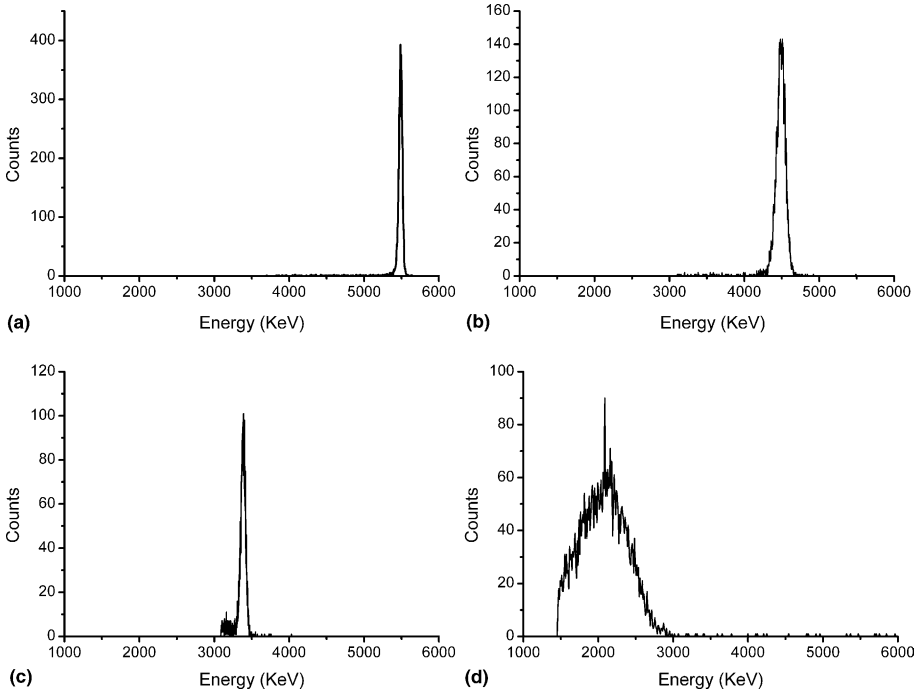

Fig. 4. The four beams of alpha-particles: (a) ^{241}Am source, (b) ^{241}Am source plus 10 μm polyethylene absorber, (c) ^{241}Am source plus 20 μm polyethylene absorber and (d) ^{241}Am source plus 30 μm polyethylene absorber.

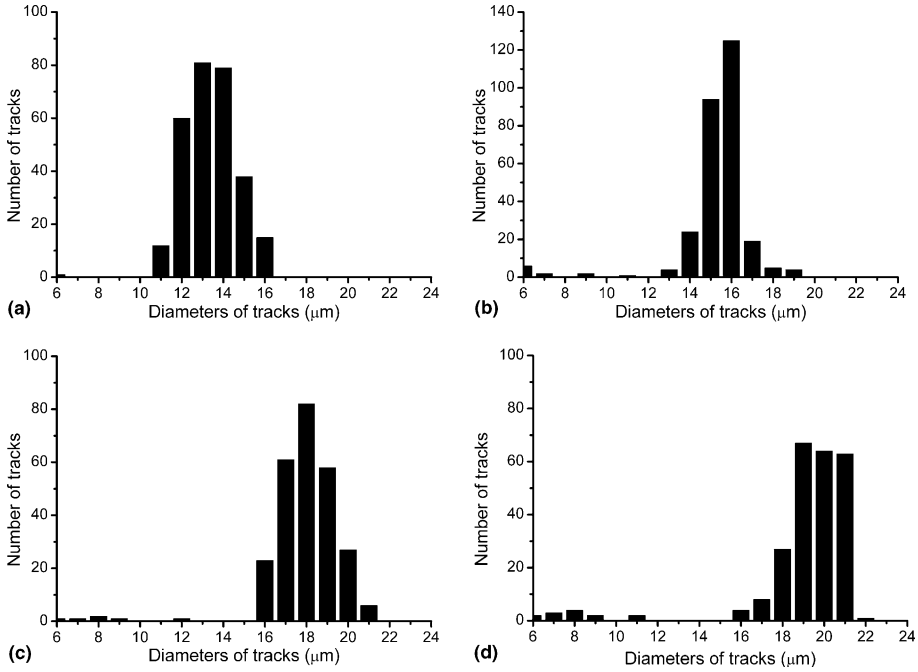

Fig. 5. The histograms represent the distribution of the diameters of tracks for 8 h CE: (a) ^{241}Am source, (b) ^{241}Am source plus 10 μm polyethylene absorber, (c) ^{241}Am source plus 20 μm polyethylene absorber and (d) ^{241}Am source plus 30 μm polyethylene absorber.

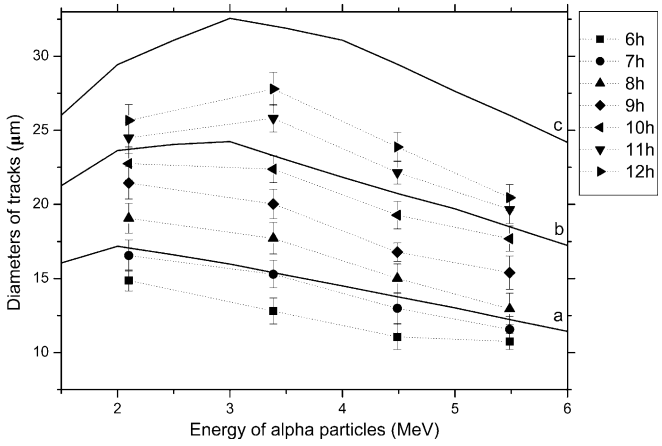

Fig. 6. The comparison between the experimental results analysed by TRIAC for different CE times (6–12 h) and the theoretical predictions for the tracks openings as function of particles energies for different CE times: (a) 7.5 μm removed layer [21], (b) 11 μm removed layer [21] and (c) 15 μm removed layer [21].

5. Conclusions

The computer code described here provides reproducible results at a scanning time of less than 3 min per image analyzed. It is easy to operate and when used in a systematic way provides reliable counting results, even when overlapping tracks exist. Unlike other codes, it does not require the definition of a brightness threshold. The system's counting performance was tested using CR39 detectors exposed in a radon-rich environment and the possibilities it offers for energy discrimination was assessed using the alpha-particles from a ^{241}Am source.

References

[1] J. Dreute, W. Trakowski, B. Schofer, C. Brectman, H. Drechel, H. Eversberg, W. Fricke, J. Beer, B. Wiegel, W. Heinrich, Nucl. Tracks 12 (1986) 261.
[2] A. Fews, Nucl. Instr. and Meth. B 72 (1992) 91.
[3] J. Molnar, S. Somogyi, S. Szilagyi, K. Spesi, Nucl. Tracks 8 (1984) 243.
[4] J. Skvarc, Informacije MIDEM 23 (1993) 201.
[5] A. Boukhair, A. Haessler, J.C. Adloff, A. Nourreddine, Nucl. Instr. and Meth. B 160 (2000) 550.
[6] N.K. Pal, S.K. Pal, Pattern Recognit. 26 (1993) 1277.
[7] R.O. Duda, P.E. Hart, D.G. Stork, Pattern Classification, Wiley-Interscience, New York, 2001.
[8] J. Canny, IEEE Trans. Pattern Anal. Mach. Intell. 8 (1986) 679.
[9] J.R. Parker, Algorithms for Image Processing and Computer Vision, John Wiley & Sons Inc., 1996.
[10] R.K.K. Yip, P.K.S. Tam, D.N.K. Leung, Pattern Recognit. 25 (1992) 1007.
[11] K.G. Ioannides, K.C. Stamoulis, C.A. Papachristodoulou, Health Phys. 79 (2000) 697.
[12] P.R. Henke, E. Benton, Nucl. Instr. and Meth. 97 (1971) 483.
[13] G. Somogyi, A.S. Szalay, Nucl. Instr. and Meth. 109 (1973) 211.
[14] G.H. Paretzke, E. Benton, P.R. Henke, Nucl. Instr. and Meth. 108 (1973) 73.
[15] G. Somogyi, Nucl. Instr. and Meth. 173 (1980) 21.
[16] M. Fromm, P. Meyer, A. Chambaudet, Nucl. Instr. and Meth. B 107 (1996) 337.
[17] R. Barillon, M. Fromm, A. Chambaudet, H. Marah, A. Sabir, Radiat. Meas. 28 (1997) 619.
[18] V. Ditlov, Radiat. Meas. 25 (1995) 89.
[19] D. Nikezic, D. Kostic, Radiat. Meas. 28 (1997) 185.
[20] D. Nikezic, Radiat. Meas. 32 (2000) 277.
[21] D. Nikezic, K.N. Yu, Radiat. Meas. 37 (2003) 39.
[22] A.P. Fews, D.L. Henshaw, Nucl. Instr. and Meth. 197 (1982) 517.